

UC Santa Cruz

UC Santa Cruz Previously Published Works

Title

Biofilm Inhibitor Taurolithocholic Acid Alters Colony Morphology, Specialized Metabolism, and Virulence of *Pseudomonas aeruginosa*

Permalink

<https://escholarship.org/uc/item/64q3t7m4>

Journal

ACS Infectious Diseases, 6(4)

ISSN

2373-8227

Authors

Condren, Alanna R
Kahl, Lisa Juliane
Boelter, Gabriela
[et al.](#)

Publication Date

2020-04-10

DOI

10.1021/acsinfecdis.9b00424

Peer reviewed



Published in final edited form as:

ACS Infect Dis. 2020 April 10; 6(4): 603–612. doi:10.1021/acsinfecdis.9b00424.

Biofilm inhibitor tauroolithocholic acid alters colony morphology, specialized metabolism, and virulence of *Pseudomonas aeruginosa*

Alanna R. Condren¹, Lisa Juliane Kahl², Gabriela Boelter³, George Kritikos³, Manuel Banzhaf³, Lars E. P. Dietrich², Laura M. Sanchez¹

¹ Department of Pharmaceutical Sciences, University of Illinois at Chicago, 833 S Wood St. Chicago, IL 60612

² Department of Biological Sciences, Columbia University, 617A Fairchild Center, New York, NY 10027

³ Institute of Microbiology & Infection and School of Biosciences, University of Birmingham, Edgbaston, Birmingham, B15 2TT, UK.

Abstract

Biofilm inhibition by exogenous molecules has been an attractive strategy for the development of novel therapeutics. We investigated the biofilm inhibitor tauroolithocholic acid (TLCA) and its effects on the specialized metabolism, virulence and biofilm formation of the clinically relevant bacterium *Pseudomonas aeruginosa* strain PA14. Our study shows that TLCA alters specialized metabolism, thereby affecting *P. aeruginosa* colony biofilm physiology. We observed an upregulation of metabolites correlated to virulence such as the siderophore pyochelin. A wax moth virulence assay confirmed that treatment with TLCA increases virulence of *P. aeruginosa*. Based on our results, we believe that future endeavors to identify biofilm inhibitors must consider how a putative lead is altering the specialized metabolism of a bacterial community to prevent pathogens from entering a highly virulent state.

Graphical Abstract

Correspondence, sanchelm@uic.edu.

Author Contributions

Wrote the paper: ARC, LK, GB, GK, MB, LD, LMS

Conceptualized the research: ARC, LMS

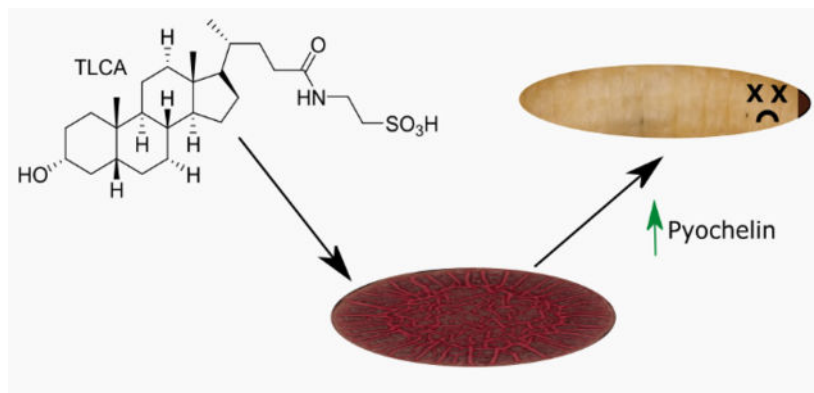
Conducted the experiments: ARC, LK, MB, GK, GB

Provided strains: LK, LD

Supervised the research: MB, LD, LMS

Supporting information

Materials and methods expanded information, strain information, molecular networking used to verify the structures identified with imaging mass spectrometry, IMS replicates, fold change HPLC analysis, mass error reports and statistical analysis reports, data availability.



Keywords

biofilms; taurochenodeoxycholic acid; bile acid; *Pseudomonas aeruginosa*; virulence

The ESKAPE pathogens (*Enterococcus faecium*, *Staphylococcus aureus*, *Klebsiella pneumoniae*, *Acinetobacter baumannii*, *Pseudomonas aeruginosa*, and *Enterobacter* species) have been deemed a severe threat, as the major cause of nosocomial infections, by evolving mechanisms to “escape” the biocidal action of antibiotics.^{1,2} The Center for Disease Control and Prevention estimates that costs related to nosocomial infections, which have increased in frequency in all countries regardless of income or industrial development, are between \$680 to \$5,683 USD on average per patient.³

P. aeruginosa, one of the ESKAPE microorganisms, is often referred to as a “ubiquitous” bacterium because of its ability to adapt to a wide variety of environments and hosts.⁴ *P. aeruginosa* can be found in the lung of cystic fibrosis patients, colonizing large open wounds of burn victims in hospitals, or invading the cornea of the human eye leading to permanent vision loss.^{5–7} *P. aeruginosa* infections are often complicated by the fact that it readily forms a multicellular aggregate known as a biofilm - a state which contributes towards its resistance to antibiotics.⁸ The minimum bactericidal concentration for cells in a biofilm state is estimated to be 10–1000 times higher than their planktonic counterparts complicating treatment of biofilm infections.⁹ Yet, there are currently no biofilm inhibitors on the market in the US.¹⁰

There are, however, several biofilm inhibitors used for *in vitro* analysis of biofilm dispersal.¹¹ One example is taurochenodeoxycholic acid (TLCA), a bile acid which efficiently inhibits biofilm formation and induces dispersal of mature *P. aeruginosa* biofilms.^{12,13} TLCA demonstrated a low micromolar biofilm inhibitory concentration (BIC₅₀) against *P. aeruginosa* at 38.4 μM compared to other lithocholic and bile acid derivatives.¹² Bile acids are a class of acidic steroids that play a physiological role in digestion by solubilizing dietary fats.¹⁴ Though bile acids are classified as detergents, the steroid control cholesterol 3-sulfate, does not inhibit biofilm formation nor do other bile acids tested at concentrations up to 1 mM. However, all lithocholic bile acids have specific bioactivity against *P. aeruginosa* which varies based on the conjugation to glycine or taurine.¹² Additionally, the reported BIC₅₀ of TLCA was in the low micromolar range while the maximum critical

micelle concentration for these bile acids ranges from 8 to 12 mM.¹⁴ *P. aeruginosa* tightly regulates biofilm formation using molecular signaling networks and a well-characterized arsenal of specialized metabolites.^{15–19} Therefore, we hypothesized that TLCA treatment induces *P. aeruginosa* to alter the production of specific specialized metabolites leading to the reported biofilm inhibition/dispersion.

We observed altered morphology of colony biofilms and changes in specialized metabolism when *P. aeruginosa* PA14 is exposed to TLCA. An increase in pyochelin production when TLCA is present lead us to perform a wax moth virulence assay which confirmed that TLCA treated cells are significantly more virulent than non-treated cells.²⁰ The observed increase in virulence led to an investigation into how TLCA may be inducing an increase in virulence factors such as pyochelin. We performed an iron starvation assay as well as mutant studies via imaging mass spectrometry (IMS) which concluded that TLCA treatment does not make *P. aeruginosa* cells sensitive to iron starvation and a knockout of the *pqsH* (*pqsH*) and *phzA1-G1 phzA2-G2* (*phz*) gene clusters also leads to an increase in pyochelin production as observed in the wild-type strain.²¹ Taken together, while TLCA has shown promising bioactivity towards biofilm inhibition, it appears that biofilm inhibition (or dispersion) ultimately leads to the bacterium becoming more virulent in a host model, which is foreshadowed by the observed alteration in specialized metabolism.

Results & Discussion

Phenazines constitute one of the most notable families of specialized metabolites produced by *P. aeruginosa*. Phenazines are redox-active compounds that have been implicated in balancing redox homeostasis in the hypoxic regions of biofilms, thereby regulating biofilm morphology.^{22–26} A phenazine-null mutant (*phz*) over produces extracellular matrix which causes *phz* mutant biofilms to have a characteristic hyper wrinkled morphology that allows for increased access to oxygen due to a higher surface area-to-volume ratio.^{26–29} To characterize the effect of TLCA on *P. aeruginosa* biofilms, we grew PA14 colonies in a colony morphology assay on solid agar supplemented with Congo Red, Coomassie Blue, and TLCA (0, 100, 250, and 1000 μ M) for five days (Figure S1). Wild type PA14 initially forms a smooth colony but initiates wrinkle structure development after 70 h (Figure 1). In contrast, a *phz* mutant showed enhanced production of biofilm matrix, leading to an earlier onset of wrinkling between 24 and 48 h. Addition of TLCA to the medium promoted a hyper-wrinkled morphology after 94 h. The colony continued to wrinkle over time, resembling the *phz* mutant (118 h; Figure 1). This morphology phenotype was also observed at lower concentrations, but it was most dramatic at 1 mM TLCA, which is a physiologically relevant concentration (Figure S1).³⁰ Based on this assay, it appears that TLCA induces matrix production, possibly by downregulating phenazines.

The putative decrease in phenazine production as indicated by the *phz*-like colony morphology in the presence of TLCA was queried alongside other changes in specialized metabolism using imaging mass spectrometry (IMS). We employed matrix-assisted laser desorption/ionization time-of-flight IMS (MALDI-TOF IMS), because it provides a robust, untargeted analysis of the specialized metabolites produced by *P. aeruginosa in situ*.^{31,32} *P. aeruginosa* colonies were grown on thin agar (2–3 mm) with the vehicle or 250 μ M of TLCA

for 48 h. The colonies and their respective agar controls were then prepared for IMS analysis. Twelve known specialized metabolites were identified and visualized from *P. aeruginosa* colonies (Figure 2). Orthogonal analytical techniques were used to confirm identities of all twelve metabolites (Figure S2). Following a combination of manual and statistical analyses using SCiLS lab, eight of the twelve specialized metabolites were observed to have significant altered regulation in the presence of TLCA ($p < 0.05$; Table S1). The specialized metabolites represent four broad classes of molecular families including the phenazines, quinolones, rhamnolipids, and siderophores. We found that the phenazines pyocyanin (PYO) and phenazine-1-carboxamide (PCN) are significantly downregulated when TLCA is present, supporting our hypothesis that TLCA exposure causes hyper-wrinkled colonies by downregulating phenazine production. We did not observe a statistically significant change in phenazine-1-carboxylic acid (PCA) production in the presence of TLCA. Since N-methylated phenazines like PYO were shown to inhibit colony wrinkling our data is consistent with TLCA affecting colony morphology by modulating phenazine production.³³

Twelve specialized metabolites produced by *P. aeruginosa* were identified and visualized. Signal intensity is displayed as a heat map and shows that exposure to TLCA altered regulation of highlighted specialized metabolites compared to control. * denotes the signal is significantly up- or down-regulated in two biological replicates within the colony and ** denotes the signal was significant over all three biological replicates ($p < 0.05$).

P. aeruginosa is reported to produce up to 50 quinolones which are specialized metabolites that play specific roles in signaling and/or virulence. For example, both 2-heptyl-4-quinolone (HHQ) and *Pseudomonas* quinolone signal (PQS) are specifically known for their signaling properties but have also demonstrated antifungal bioactivity.^{34–40} The N-oxide quinolone, 4-hydroxy-2-heptylquinoline-N-oxide (HQNO), has recently been shown to have antimicrobial activity towards Gram-positive bacteria and contributes to *P. aeruginosa*'s virulence.^{34–39} When *P. aeruginosa* was treated with TLCA, we observed a significant upregulation of HHQ, PQS, and 4-hydroxy-2-nonylquinoline (HNQ) in the *P. aeruginosa* colony. PQS is a well-characterized signaling molecule in *P. aeruginosa* quorum sensing cascade.⁴¹ Though IMS is a valuable tool for identifying and visualizing the chemical composition of a sample, it cannot differentiate between constitutional isomers like HQNO and PQS (m/z 260; Figure 2). In order to differentiate these two metabolites, we used a combination of tandem mass spectrometry and knockout mutants to demonstrate that PQS was represented by the signal that is retained in the colony (center, upregulated) and HQNO corresponds to the signal that was excreted into the agar (outer signal, downregulated). HHQ and PQS are well established signaling molecules that are required for phenazine production in *Pseudomonas aeruginosa*. However, since we observed decreased phenazine levels despite an increase in quinolone production⁴² our results suggest that TLCA is attenuating phenazine production in a quinolone-independent manner.

Based on the IMS analyses, treatment of TLCA seems to induce the production of biosurfactants. Surfactants, such as rhamnolipids, are amphipathic small molecules that *P. aeruginosa* produces to increase surface adhesion and motility.⁴³ Rha-Rha-C10-C10 and Rha-Rha-C12-C10/C10-C12 were produced at elevated levels after treatment with TLCA

(Figure 2). However, while the upregulation was not determined to be statistically significant over all biological replicates, the trend observed is worth noting. In colony biofilms, TLCA markedly increases matrix production and leads to increased spreading and wrinkling. This wrinkly spreader phenotype is reminiscent of the phenazine-null mutant as seen in Figure 1.

In addition to quinolones and phenazines, we detected changes in the levels of the siderophore pyochelin. Siderophores are iron chelators that allow bacteria to acquire iron from the surrounding environment.⁴⁴ Siderophores have been known to sequester iron from host proteins and simultaneously act as signals for biofilm development.¹⁷ The IMS results show a significant upregulation of pyochelin in the presence of TLCA (Figure 2). Pyochelin is produced by the biosynthetic pathway *pchA-I* which is activated by the presence of both iron and the ferric uptake regulator (Fur).¹⁷ Additionally, previous work has shown that an increase in iron-bound PQS can indirectly increase siderophore production by activating the siderophore gene clusters *pvd* and *pch*; our IMS experiments with TLCA treatment of wild-type PA14 are in line with these results (Figure 2).⁴⁵ Siderophores have antimicrobial activity and contribute to virulence.^{46,47} Hence, the TLCA-dependent upregulation of pyochelin raised the question of whether TLCA-treatment induced *P. aeruginosa* to be hypervirulent.

Many bacteria, like the ESKAPE pathogens, exhibit distinct lifestyle states depending on surrounding environmental factors. Chua *et al.* recently described characteristics of the dispersed cell state using sodium nitroprusside (SNP) as a biofilm-dispersing agent.²¹ They found that dispersed cells are characterized by altered physiology, increased virulence against macrophages and *C. elegans*, and extreme sensitivity to iron starvation.²¹ Having observed an increase in pyochelin production when exposing *P. aeruginosa* to TLCA (Figure 2), we sought to determine if TLCA treated cells were hypervirulent using a *Galleria mellonella* (greater wax moth) larvae virulence assay.

G. mellonella larvae have been shown to be an ideal model for studying microbial pathogenesis of several ESKAPE pathogens since they are easily infected, inexpensive, and produce a similar immune response as vertebrates and mammals.^{48–52} In the *G. mellonella* model, the potency of treatment is measured via a Kaplan-Meier curve, therefore a shift at the 50% survival rate compared to the appropriate control will indicate increased or decreased virulence of *P. aeruginosa*.⁵³ To observe how TLCA and SNP treatment altered virulence of *P. aeruginosa* infected larvae, TLCA or SNP were injected with *P. aeruginosa* and larvae survival was monitored for 25 h. Treatment of uninfected larvae with either SNP or TLCA did not affect larvae survival (Figure 3; Table S2). Within 15 h, 50% of larvae infected with *P. aeruginosa* succumbed to infection and treatment with SNP or TLCA led to a significant decrease in survival with 50% of the larvae succumbing to infection 2 h earlier than the infected control group (Figure 3; $p < 0.05$). These results indicate that TLCA treatment increases virulence, mimicking what was previously reported from SNP treatment.²² Given the high dose of TLCA administered we also sought to control for an immunological response. Larvae were treated with taurocholic acid (TCA), a derivative of TLCA which has been previously shown to have no biofilm inhibition against *P. aeruginosa*.¹⁸ Treatment with TCA altered survival slightly however only TLCA treatment caused a significant increase in virulence compared to control group (Figure S3A). This suggests that

treatment with bile acids induces an innate immunological response but the observed increase in virulence from TLCA treatment is significant compared to TCA treatment or control group.

In continuing to explore how specialized metabolites impact virulence, we used the *phz* mutant in the wax moth assay. We observed the *phz* mutant takes longer than WT to reduce the population to 50%, therefore, the *phz* mutant is intrinsically less virulent (Figure S3B). TLCA treatment of the *phz* mutant infected larvae induce a significant increase in virulence compared to the control (Figure S3B; $p < 0.05$), however, TCA treatment induced the same increase in virulence. This similarity in response to both bile acids indicates that the observed shift in the survival curve of the *phz* mutant is due to an immunological response from the bile acids. Based on our *in vivo* assays, WT PA14 cells treated with TLCA are significantly more virulent, and TLCA treatment is linked to specialized metabolism since the increase in virulence was lost when the *phz* mutant was tested.

In a previous report, SNP-dispersed *P. aeruginosa* PAO1 cells resulted in decreased production of the siderophore pyoverdine and also showed a sensitivity to iron starvation when competing with exogenous iron chelator DIPY.²² We were unable to detect pyoverdine in either the wild type or TLCA-treated *P. aeruginosa* PA14 via mass spectrometry, but we were able to detect pyochelin in our IMS experiments which Chua *et al.* did not measure (Figure 2). Having confirmed that TLCA treatment increases virulence in *P. aeruginosa*, we next tested whether *P. aeruginosa* TLCA-treated cells would also be sensitive to iron stress even with increased pyochelin production. Therefore, we recapitulated the iron starvation assay performed by Chua *et al.* to determine if TLCA exposure induced sensitivity to iron starvation as shown previously for SNP-dispersed cells.

Iron starvation was induced by exposing PA14 cells to the iron chelator 2'2-bipyridine (DIPY; Figure 4). This assay was performed with TLCA or SNP treated cells, which were generated using two different methods: 1) from pellicles (biofilms grown at the air-liquid interface in standing liquid cultures; Figure 4A–C), and 2) planktonic cells (shaken liquid cultures; Figure 4D–F). Treatment of *P. aeruginosa* PA14 with either TLCA or SNP does not alter proliferation compared to the DIPY control (Figure 4B). Regardless of agent used for treatment, *P. aeruginosa* PA14 cells do not show an increase in sensitivity to iron starvation (Figure S4). Therefore, TLCA and SNP treatment does not increase *P. aeruginosa* PA14's sensitivity to iron starvation. The same trend occurred with *P. aeruginosa* PA14 *phz* mutant (Figure 4C).

Using WT PA14 planktonic cells, we observe no change in growth regardless of condition (Figure 4E). Interestingly, TLCA treatment of the *phz* mutant planktonic cells showed a significant increase in sensitivity compared to SNP treated cells (Figure 4F). Based on our data, dispersed biofilm cells and WT planktonic cells show no sensitivity to iron starvation. However, planktonic cells of the *phz* mutant show significant sensitivity when biofilm formation is inhibited via TLCA treatment. This result agrees with our hypothesis that TLCA is altering the specialized metabolism of PA14 and phenazines may help alleviate sensitivity to iron starvation during TLCA treatment since phenazines are capable of carrying out oxidation and reduction of iron species to increase bioavailability.²⁷ With our

previous morphology assay and IMS experiments, the iron starvation assay confirms that TLCA treatment likely effects phenazine production which leads to altered morphology and metabolism in response to biofilm inhibition from an exogenous small molecule treatment.

Of note, we do not observe the same sensitivity of SNP treatment with iron starvation as reported by Chua *et al.* which is likely due to the difference in strains used for this assay (PA14 vs PAO1). The discrepancy in iron starvation sensitivity between SNP and TLCA might be attributed to different pyoverdine production capabilities of these strains. Though we were unable to detect pyoverdine in our IMS analysis, we would speculate that iron starvation might be prevented by the increased production of pyochelin in colony biofilms that were treated with TLCA (Figure 2). Despite their differing effects on iron starvation sensitivity, both SNP and TLCA have previously been shown to readily disperse biofilms, likely through different mechanisms of action.^{18,22} SNP, a nitric oxide donor, has been shown to disperse mature biofilms by producing nitrosative stress inside of the biofilm structure.²¹ Since TLCA cannot act as a nitric oxide donor and it does not cause cell lysis, TLCA must act via an alternative mechanism to disperse biofilms.¹⁸ This supports our hypothesis that TLCA's bioactivity is achieved through inducing changes in *P. aeruginosa*'s specialized metabolism.

PQS is a major quorum sensing signal and iron-bound PQS upregulates siderophore production.⁴⁵ The increase in pyochelin production *in situ* and the enhanced virulence *in vivo* lead us to investigate the contribution of the *pqs* gene cluster to the TLCA-mediated effect. We tested four mutants with deletions in quinolone and phenazine biosynthetic genes: *pqsA-C*, *pqsH*, *pqsL*, and *phz*. *pqsA-C* does not produce any quinolones, while *pqsH* cannot produce PQS and *pqsL* cannot produce N-oxide quinolones such as HQNO.^{42,48,49} The phenazine-null mutant, *phz*, is a double-deletion of the two redundant core phenazine biosynthetic gene clusters *phzA1-G1* and *phzA2-G2*.^{42,48,49} Using IMS, we investigated if any of the four mutants would recapitulate the TLCA-dependent increase in pyochelin production that we observed for the WT. No variation in pyochelin production for *pqsA-C* and *pqsL* mutants was found, while *pqsH* mutant produced significantly more pyochelin in response to TLCA, mimicking the trend observed in the WT ($p < 0.05$; Figure S5). This result puts into question our earlier assumption that PQS and pyochelin production are positively correlated. We also observed a significant increase in pyochelin production in the *phz* mutant (Figure S5). Previous work has shown that increasing PCA concentrations allows PA14 siderophore-null mutants to still develop biofilms and sequester iron.⁵⁰ This may be due to phenazine's ability to mediate the reduction of Fe(III) to the bioavailable Fe(II).⁵⁰ *pqsH* and *phz* gene clusters are necessary for phenazine production, hence a decrease or lack of phenazine production caused by TLCA treatment might be responsible for the observed increase in pyochelin production (Figures 2 & S5).

Since our IMS results were inconclusive regarding the effect of TLCA on PCA production in colony biofilms (Figure 2), we subjected bacterial colony extracts from wild-type PA14, *pqsH*, and the *phz* mutant to an HPLC analysis to measure fold change across biological (N=3) and technical replicates (n=3) (Figure 5A). When considering fold changes greater than ± 1 , PCA production was not altered by TLCA exposure in the wild type and *pqsH* strains (not produced by the *phz* mutant). When monitoring pyochelin production, only

TLCA treatment of the *phz* mutant showed a fold change increase in pyochelin production compared to control (+2.20) (Figure 5B). When the *pqsH* mutant is complemented (*pqsH::pqsH*) there is increased production of pyochelin compared to the wild-type regardless of whether the colony is TLCA-treated or not (Table S3). There was no notable difference in production of pyochelin in the complementation strain whether it was TLCA-treated or not, which recapitulates the wild-type data. Though the fold change of PCA and pyochelin was comparable in both wild-type PA14 and *pqsH*, the change in the production of these two metabolites in the phenazine-null mutant, *phz*, suggests that a lack of phenazine production is correlated to the observed increase in pyochelin production from cells exposed to TLCA.

Conclusion

In this study we demonstrate that the mammalian endogenous enteric metabolite, TLCA, can alter colony morphology, specialized metabolism, and virulence of *P. aeruginosa*. Our biological and chemical studies confirm what is already known about TLCA's bioactivity and offers insight into the chemical communication occurring between the cells upon treatment with a known biofilm inhibitor. TLCA-treated cells are not sensitive to iron starvation, as previously reported for the biofilm-dispersing agent SNP, however treatment with either agent induces a significant increase in virulence *in vivo*, implying that the mechanism of action of the two biofilm inhibitors is different. Our IMS analysis of mutant strains revealed that when exposed to TLCA, a lack of PQS (*pqsH*) or phenazine production (*phz*) lead to an increase in pyochelin production, matching the results observed in our colony morphology and IMS WT experiments. Therefore, PQS or iron-bound PQS is not responsible for activating the *pchA-I* gene cluster (Figure 6A). IMS analysis highlighted that a significant increase in pyochelin production was observed in the *phz* mutant confirming that TLCA treatment not only affects phenazine production but could also play a role in the observed increased pyochelin production when TLCA is present (Figure 6B). Though these results are not conclusive regarding the mechanism of TLCA since biofilm inhibition and dispersal cannot be tested using colony biofilms as a model system, it does support the hypothesis that TLCA is acting as an environmental cue to induce *P. aeruginosa* to alter its metabolic signaling throughout the bacterial community.

More work is needed to determine the mechanism of action of TLCA, but our work shows that TLCA-treated *P. aeruginosa* bacterial communities increase the production of virulence factors, such as pyochelin, *in vitro* and induced hypervirulence *in vivo*. Others have documented similar phenomena by reporting an increase in virulence *in vivo* as a consequence of treatment with a biofilm inhibitor in organisms such as, Group A *Streptococcus*, *Vibrio cholerae*, and *Candida albicans*.⁵¹⁻⁵⁵ Based on previous literature, our work supports that future investigations should consider the chemical environment within a biofilm, and that biofilm inhibition as a treatment strategy should be closely monitored for undesired side effects, such as increased virulence.

Methods

TLCA stock solution preparation

Taurolithocholic acid was purchased from Sigma Aldrich (98%). A 0.5 M stock solution was made by dissolving TLCA in methanol. This solution was then sterile filtered with a 0.22 μm sterile filter and stored at -80°C .

Colony Morphology Studies

Liquid agar was prepared by autoclaving 1% tryptone (Teknova), 1% agar (Teknova) mixture. The liquid agar was cooled to 60°C and Congo Red (EMD; final concentration 40 $\mu\text{g}/\text{mL}$) and Coomassie Blue (EMD; final concentration: 20 $\mu\text{g}/\text{mL}$) were added. TLCA stock solution, dissolved in MeOH, was vortexed for 2–3 min until clear. TLCA was added to liquid agar, different amounts were added to reach the final concentrations of 100 μM , 250 μM , and 1 mM TLCA. 60 mL of liquid agar mixture was poured into square plates (LDP, 10 cm x 10 cm x 1.5 cm) and left to solidify for ~18–24 h. Precultures of *P. aeruginosa* PA14 were grown in LB for 12–16 h at 37°C while shaking at 250 rpm. Subcultures were prepared as 1:100 dilutions of precultures into fresh LB media and shaking for 2.5 h at 37°C , at which point all subcultures had reached mid-exponential phase (optical density of ~0.4–0.6 at 500 nm). Morphology plates were dried for 20–30 min and 10 μL spots of subculture were spotted onto a morphology plate, with not more than four colonies per plate. Colony biofilms were grown at 25°C and high humidity (+90%) for up to 5 d. Images were taken every 24 h with a Keyence VHX-1000 microscope.

Imaging mass spectrometry experiments

TLCA and the respective vehicle (MeOH) were added into liquid agar prior to plating. LB agar was autoclaved and cooled to 55°C before adding TLCA. The final concentration of TLCA in each agar plate was 250 μM . Plates were stored in 4°C refrigerator until needed. *P. aeruginosa* PA14 was plated on Bacto LB agar and grown overnight at 30°C . A colony from the plate was then used to inoculate a 5 mL LB liquid culture of *P. aeruginosa* and grown overnight at 30°C shaking at 225 rpm. Overnight liquid cultures (5 μL) was spotted on thin agar plates (10 mL of agar in 90 mm plate) embedded with either TLCA or the vehicle (MeOH) and incubated for 48 h at 30°C . Humidity/moisture was removed from environment during growth by placing a small amount of DrieRite in the incubator. Following 48 h of growth, colonies were excised from agar plates using a razor blade and transferred to an MSP 96 target ground steel target plate (Bruker Daltonics). An optical image of the colonies on the target plate was taken prior to matrix application. A 53 μm stainless steel sieve (Hogentogler Inc) was used to coat the steel target plate and colonies with MALDI matrix. The MALDI matrix used for the analysis was a 1:1 mixture of recrystallized α -cyano-4-hydroxycinnamic acid (CHCA) and 2,5-dihydroxybenzoic acid (DHB) (Sigma). The plate was then placed in an oven at 37°C for approximately 4 h or until the agar was fully desiccated. After 4 h, excess matrix was removed from target plate and sample with a stream of air. Another optical image was taken of the desiccated colonies on the target plate. The target plate and desiccated colony were then introduced into the MALDI-TOF mass spectrometer (Bruker Autoflex Speed) and analyzed with FlexControl v.3.4 and FlexImaging v.4.1 software. The detector gain and laser power were set at $3.0\times$ and 41% respectively.

Range of detection was from 100 Da to 3,500 Da with ion suppression set at 50 Da in positive reflectron mode. The raster size was set to 500 μm and the laser was set to 200 shots per raster point at medium (3) laser size.

Statistical analysis of Imaging Data

SCiLS software (Bruker, version 2015b) was used to run statistical analysis of raw imaging data. Settings for analysis was as follows: Normalization: root mean square (RMS), error: ± 0.2 Da, and weak denoising for segmentation. Using “Find Discriminative Values (ROC)” for unbiased analysis, PA14 control colony was selected as class 1 and TLCA treated colony as class 2 and SCiLS identified signals that were significantly upregulated in class 1 (MeOH control colony) with a threshold of 0.75 corresponding to a Pearson correlation of $p < 0.05$. In our report, these signals are referred to as “downregulated” since they have a higher intensity in the control. The same analysis was performed with the classes flipped to identify signals that were upregulated in TLCA condition. Statistical analysis was completed after calculating mass error (Table S4) of three biological replicates (N=3) (Figures S6–8) and signals were only considered significant if altered regulation was observed in two or more replicates.

Iron Stress Tolerance Assay

The protocol for the iron stress tolerance assay used was exactly as described by Chua *et al.*,²¹ with the exceptions that strain PA14 rather than PAO1 and a 1 mM of TLCA and 2'-bipyridine (DIPY) were used. The OD at 600 nm of each liquid culture was measured every 15 min for 16 h.

Galleria mellonella treatment assays

Galleria mellonella larvae (greater wax moth) were purchased from TrueLarv UK Ltd. or Livefoods, UK and stored at 15°C prior to use. The assay was performed as described previously,⁵⁶ except for the following differences: PA14 wild-type (WT) cells were grown exponentially for 2 h, washed with PBS buffer and adjusted to an $\text{OD}_{(600)}$ of 0.1. The PA14 culture was further diluted with PBS and plated to determine the CFU of the inoculation suspension. Larvae were inoculated with 20 μL of a 2.5×10^3 CFU/mL solution and 20 μL of compound or PBS. The final concentration of TLCA and sodium nitroprusside (SNP) was 250 μM . For controls, uninfected larvae were administered the same compound dose to monitor for toxicity. In parallel one group of larvae received sterile PBS injections to control for unintentional killing by the injections. Survival of a larvae was determined by the ability to respond to external stimuli (poking). To increase robustness of the *G. mellonella* treatment assay several, independent experiments were pooled to draw conclusions. All raw data can be found in supplementary data set 1. Larvae survival was estimated using the Kaplan-Meier estimator.⁵⁷ Survival estimates were subsequently compared using the log-rank test.⁵⁸ Resulting p-values were corrected using the Benjamini-Hochberg method (Tables S2 & S5).

59

pqs mutants IMS analysis

Mutants proceeded through the same protocol as the WT (PA14) bacterial colonies. IMS sample prep and experimentation was completed at the same settings as described in “Imaging mass spectrometry experiments” section. Statistical analysis was completed after calculating mass error (Table S6–S10) of three biological replicates (N=3) and signals were only considered significant if altered regulation was observed in two or more replicates.

PQS complementation

The complementation strains *P. aeruginosa* PA14 *pqsA-C::pqsA-C*, *pqsH::pqsH*, and *pqsL::pqsL* were constructed as described in Jo *et al.* [57]. Primers LD1 & LD4, LD168 & LD171, and LD9 & LD12 were used to amplify the *pqsA-C*, *pqsH* and *pqsL* genes, respectively (Table S11). Correct constructs were confirmed by PCR and sequencing and complemented into the original deletion site, following the same procedure as for deletion.

Bacterial Extraction for PCA and PCH Fold-change

Bacterial growth for quantification proceeded exactly as described in “Imaging mass spectrometry experiments”. Each strain (PA14 WT, *pqsA-C*, *pqsH*, *phz*, *pqsA-C::pqsA-C*, and *pqsH::pqsH*) was plated in duplicate. After 48 h, colonies and surrounding agar were excised, transferred, and extracted with MeOH. Total weights of each sample dry extract was used to achieve a 10 mg/mL solution of each extract for HPLC analysis (N=3, n=3).

PCA and PCH Fold-change analysis

PCA standard was purchased from ChemScience (>97%). An HPLC method previously described by Adler *et al.* was used on an Agilent 1260 Infinity to isolate and identify PCA through retention time matching with standard (32.5 min at 250 nm; Figure S9) with a Phenomenex C18 analytical column (150 × 4.6 mm; 5 μm) and a flow rate of 0.5 mL/min.⁶⁰ Area under the curve (AUC) was used to quantify fold-change between PA14 WT and other strains/conditions. For PCH fold-change quantification, a gradient of 10%–85% ACN (0.1% TFA) and H₂O (0.1% TFA) over 25 min with the two PCH stereoisomers (pyochelin I and II) eluting at 16.0 & 16.2 min respectively at 210 nm (Figure S10). Area reported for fold change analysis was achieved by combining the AUC of the peaks for pyochelin I and II. Fold-change analysis was determined by averaging the AUC's from three independent biological cultures (N=3), with three technical replicates (n=3), and compared to PA14 WT with no TLCA (control).

Supplementary Material

Refer to Web version on PubMed Central for supplementary material.

Acknowledgements

We thank Drs. Atul Jain and Terry Moore for assisting with the recrystallization of the MALDI matrices, Dr. Michael Federle for access to Biotek plate reader, and Dr M. Lisandra Zepeda Mendoza for assistance with statistics. Funding was provided by Grant K12HD055892 from the National Institute of Child Health and Human Development (NICHD) and the National Institutes of Health Office of Research on Women's Health (ORWH) (L.M.S.); University of Illinois at Chicago Startup Funds (L.M.S.); American Society for Pharmacognosy research

startup grant (L.M.S.); NIH/NIAID grant R01AI103369 and an NSF CAREER award (L.E.P.D). ARC was supported in part by the National Science Foundation Illinois Louis Stokes Alliance for Minority Participation Bridge to the Doctorate Fellowship (grant number 1500368) and a UIC Abraham Lincoln retention fellowship.

References

- (1). Rice LB Federal Funding for the Study of Antimicrobial Resistance in Nosocomial Pathogens: No ESKAPE. *J. Infect. Dis.* 2008, 197 (8), 1079–1081. [PubMed: 18419525]
- (2). Rice LB Progress and Challenges in Implementing the Research on ESKAPE Pathogens. *Infect. Control Hosp. Epidemiol.* 2010, 31 Suppl 1, S7–S10. [PubMed: 20929376]
- (3). Kouchak F; Askarian M Nosocomial Infections: The Definition Criteria. *Iran. J. Med. Sci.* 2012, 37 (2), 72–73. [PubMed: 23115435]
- (4). Kramer A; Schwebke I; Kampf G How Long Do Nosocomial Pathogens Persist on Inanimate Surfaces? A Systematic Review. *BMC Infect. Dis.* 2006, 6, 130. [PubMed: 16914034]
- (5). Spencer WH *Pseudomonas Aeruginosa* Infections of the Eye. *Calif. Med.* 1953, 79 (6), 438–443. [PubMed: 13106731]
- (6). Norbury W; Herndon DN; Tanksley J; Jeschke MG; Finnerty CC Infection in Burns. *Surg. Infect.* 2016, 17 (2), 250–255.
- (7). Finch S; McDonnell MJ; Abo-Leyah H; Aliberti S; Chalmers JD A Comprehensive Analysis of the Impact of *Pseudomonas Aeruginosa* Colonization on Prognosis in Adult Bronchiectasis. *Ann. Am. Thorac. Soc.* 2015, 12 (11), 1602–1611. [PubMed: 26356317]
- (8). Hall CW; Hinz AJ; Gagnon LB-P; Zhang L; Nadeau J-P; Copeland S; Saha B; Mah T-F *Pseudomonas Aeruginosa* Biofilm Antibiotic Resistance Gene *ndvB* Expression Requires the RpoS Stationary-Phase Sigma Factor. *Appl. Environ. Microbiol.* 2018, 84 (7). 10.1128/AEM.02762-17.
- (9). Wu H; Moser C; Wang H-Z; Høiby N; Song Z-J Strategies for Combating Bacterial Biofilm Infections. *Int. J. Oral Sci.* 2015, 7 (1), 1–7. [PubMed: 25504208]
- (10). Stewart PS Prospects for Anti-Biofilm Pharmaceuticals. *Pharmaceuticals* 2015, 8 (3), 504–511. [PubMed: 26343685]
- (11). Rabin N; Zheng Y; Opoku-Temeng C; Du Y; Bonsu E; Sintim HO Agents That Inhibit Bacterial Biofilm Formation. *Future Med. Chem.* 2015, 7 (5), 647–671. [PubMed: 25921403]
- (12). Sanchez LM; Cheng AT; Warner CJA; Townsley L; Peach KC; Navarro G; Shikuma NJ; Bray WM; Riener RM; Yildiz FH; Linington RG Biofilm Formation and Detachment in Gram-Negative Pathogens Is Modulated by Select Bile Acids. *PLoS One* 2016, 11 (3), e0149603. [PubMed: 26992172]
- (13). Sanchez LM; Wong WR; Riener RM; Schulze CJ; Linington RG Examining the Fish Microbiome: Vertebrate-Derived Bacteria as an Environmental Niche for the Discovery of Unique Marine Natural Products. *PLoS One* 2012, 7 (5), e35398. [PubMed: 22574119]
- (14). Monte MJ; Marin JJG; Antelo A; Vazquez-Tato J Bile Acids: Chemistry, Physiology, and Pathophysiology. *World J. Gastroenterol.* 2009, 15 (7), 804–816. [PubMed: 19230041]
- (15). Mukherjee S; Moustafa DA; Stergioula V; Smith CD; Goldberg JB; Bassler BL The PqsE and RhlR Proteins Are an Autoinducer Synthase-Receptor Pair That Control Virulence and Biofilm Development in *Pseudomonas Aeruginosa*. *Proc. Natl. Acad. Sci. U. S. A.* 2018, 115 (40), E9411–E9418. [PubMed: 30224496]
- (16). Heeb S; Fletcher MP; Chhabra SR; Diggle SP; Williams P; Cámara M Quinolones: From Antibiotics to Autoinducers. *FEMS Microbiol. Rev.* 2011, 35 (2), 247–274. [PubMed: 20738404]
- (17). Banin E; Vasil ML; Greenberg EP Iron and *Pseudomonas Aeruginosa* Biofilm Formation. *Proc. Natl. Acad. Sci. U. S. A.* 2005, 102 (31), 11076–11081. [PubMed: 16043697]
- (18). Cezairliyan B; Vinayavekhin N; Grenfell-Lee D; Yuen GJ; Saghatelian A; Ausubel FM Identification of *Pseudomonas Aeruginosa* Phenazines That Kill *Caenorhabditis Elegans*. *PLoS Pathog.* 2013, 9 (1), e1003101. [PubMed: 23300454]
- (19). Das T; Kutty SK; Tavallaie R; Ibugo AI; Panchompoo J; Sehar S; Aldous L; Yeung AWS; Thomas SR; Kumar N; Gooding JJ; Manfield M Phenazine Virulence Factor Binding to

Extracellular DNA Is Important for *Pseudomonas Aeruginosa* Biofilm Formation. *Sci. Rep.* 2015, 5, 8398. [PubMed: 25669133]

- (20). Barraud N; Hassett DJ; Hwang S-H; Rice SA; Kjelleberg S; Webb JS Involvement of Nitric Oxide in Biofilm Dispersal of *Pseudomonas Aeruginosa*. *J. Bacteriol.* 2006, 188 (21), 7344–7353. [PubMed: 17050922]
- (21). Chua SL; Liu Y; Yam JKH; Chen Y; Vejborg RM; Tan BGC; Kjelleberg S; Tolker-Nielsen T; Givskov M; Yang L Dispersed Cells Represent a Distinct Stage in the Transition from Bacterial Biofilm to Planktonic Lifestyles. *Nat. Commun.* 2014, 5, 4462. [PubMed: 25042103]
- (22). Recinos DA; Sekedat MD; Hernandez A; Cohen TS; Sakhtah H; Prince AS; Price-Whelan A; Dietrich LEP Redundant Phenazine Operons in *Pseudomonas Aeruginosa* Exhibit Environment-Dependent Expression and Differential Roles in Pathogenicity. *Proc. Natl. Acad. Sci. U. S. A.* 2012, 109 (47), 19420–19425. [PubMed: 23129634]
- (23). Price-Whelan A; Dietrich LEP; Newman DK Pyocyanin Alters Redox Homeostasis and Carbon Flux through Central Metabolic Pathways in *Pseudomonas Aeruginosa* PA14. *J. Bacteriol.* 2007, 189 (17), 6372–6381. [PubMed: 17526704]
- (24). Price-Whelan A; Dietrich LEP; Newman DK Rethinking “Secondary” Metabolism: Physiological Roles for Phenazine Antibiotics. *Nat. Chem. Biol.* 2006, 2 (2), 71–78. [PubMed: 16421586]
- (25). Mentel M; Ahuja EG; Mavrodi DV; Breinbauer R; Thomashow LS; Blankenfeldt W Of Two Make One: The Biosynthesis of Phenazines. *Chembiochem* 2009, 10 (14), 2295–2304. [PubMed: 19658148]
- (26). Okegbe C; Fields BL; Cole SJ; Beierschmitt C; Morgan CJ; Price-Whelan A; Stewart RC; Lee VT; Dietrich LEP Electron-Shuttling Antibiotics Structure Bacterial Communities by Modulating Cellular Levels of c-Di-GMP. *Proc. Natl. Acad. Sci. U. S. A.* 2017, 114 (26), E5236–E5245. [PubMed: 28607054]
- (27). Briard B; Bomme P; Lechner BE; Mislin GLA; Lair V; Prévost M-C; Latgé J-P; Haas H; Beauvais A *Pseudomonas Aeruginosa* Manipulates Redox and Iron Homeostasis of Its Microbiota Partner *Aspergillus Fumigatus* via Phenazines. *Sci. Rep.* 2015, 5, 8220. [PubMed: 25665925]
- (28). Wang Y; Newman DK Redox Reactions of Phenazine Antibiotics with Ferric (hydr)oxides and Molecular Oxygen. *Environ. Sci. Technol.* 2008, 42 (7), 2380–2386. [PubMed: 18504969]
- (29). Ramos I; Dietrich LEP; Price-Whelan A; Newman DK Phenazines Affect Biofilm Formation by *Pseudomonas Aeruginosa* in Similar Ways at Various Scales. *Res. Microbiol.* 2010, 161 (3), 187–191. [PubMed: 20123017]
- (30). Hofmann AF; Eckmann L How Bile Acids Confer Gut Mucosal Protection against Bacteria. *Proc. Natl. Acad. Sci. U. S. A.* 2006, 103 (12), 4333–4334. [PubMed: 16537368]
- (31). Cleary JL; Condren AR; Zink KE; Sanchez LM Calling All Hosts: Bacterial Communication in Situ. *Chem* 2017, 2 (3), 334–358. [PubMed: 28948238]
- (32). Galey MM; Sanchez LM Spatial Analyses of Specialized Metabolites: The Key to Studying Function in Hosts. *mSystems* 2018, 3 (2). 10.1128/mSystems.00148-17.
- (33). Sakhtah H; Koyama L; Zhang Y; Morales DK; Fields BL; Price-Whelan A; Hogan DA; Shepard K; Dietrich LEP The *Pseudomonas Aeruginosa* Efflux Pump MexGHI-OpmD Transports a Natural Phenazine That Controls Gene Expression and Biofilm Development. *Proc. Natl. Acad. Sci. U. S. A.* 2016, 113 (25), E3538–E3547. [PubMed: 27274079]
- (34). Filkins LM; Graber JA; Olson DG; Dolben EL; Lynd LR; Bhuju S; O’Toole GA Coculture of *Staphylococcus Aureus* with *Pseudomonas Aeruginosa* Drives *S. Aureus* towards Fermentative Metabolism and Reduced Viability in a Cystic Fibrosis Model. *J. Bacteriol.* 2015, 197 (14), 2252–2264. [PubMed: 25917910]
- (35). Phelan VV; Moree WJ; Aguilar J; Cornett DS; Koumoutsi A; Noble SM; Pogliano K; Guerrero CA; Dorrestein PC Impact of a Transposon Insertion in *phzF2* on the Specialized Metabolite Production and Interkingdom Interactions of *Pseudomonas Aeruginosa*. *J. Bacteriol.* 2014, 196 (9), 1683–1693. [PubMed: 24532776]
- (36). Machan ZA; Taylor GW; Pitt TL; Cole PJ; Wilson R 2-Heptyl-4-Hydroxyquinoline N-Oxide, an Antistaphylococcal Agent Produced by *Pseudomonas Aeruginosa*. *J. Antimicrob. Chemother.* 1992, 30 (5), 615–623. [PubMed: 1493979]

- (37). Hoffman LR; Déziel E; D'Argenio DA; Lépine F; Emerson J; McNamara S; Gibson RL; Ramsey BW; Miller SI Selection for *Staphylococcus Aureus* Small-Colony Variants due to Growth in the Presence of *Pseudomonas Aeruginosa*. *Proc. Natl. Acad. Sci. U. S. A.* 2006, 103 (52), 19890–19895. [PubMed: 17172450]
- (38). Biswas L; Biswas R; Schlag M; Bertram R; Götz F Small-Colony Variant Selection as a Survival Strategy for *Staphylococcus Aureus* in the Presence of *Pseudomonas Aeruginosa*. *Appl. Environ. Microbiol.* 2009, 75 (21), 6910–6912. [PubMed: 19717621]
- (39). Voggu L; Schlag S; Biswas R; Rosenstein R; Rausch C; Götz F Microevolution of Cytochrome *Bd* Oxidase in *Staphylococci* and Its Implication in Resistance to Respiratory Toxins Released by *Pseudomonas*. *J. Bacteriol.* 2006, 188 (23), 8079–8086. [PubMed: 17108291]
- (40). Kim K; Kim YU; Koh BH; Hwang SS; Kim S-H; Lépine F; Cho Y-H; Lee GR HHQ and PQS, Two *Pseudomonas Aeruginosa* Quorum-Sensing Molecules, down-Regulate the Innate Immune Responses through the Nuclear Factor-kappaB Pathway. *Immunology* 2010, 129 (4), 578–588. [PubMed: 20102415]
- (41). Häussler S; Becker T The *Pseudomonas* Quinolone Signal (PQS) Balances Life and Death in *Pseudomonas Aeruginosa* Populations. *PLoS Pathog.* 2008, 4 (9), e1000166. [PubMed: 18818733]
- (42). Gallagher LA; McKnight SL; Kuznetsova MS; Pesci EC; Manoil C Functions Required for Extracellular Quinolone Signaling by *Pseudomonas Aeruginosa*. *J. Bacteriol.* 2002, 184 (23), 6472–6480. [PubMed: 12426334]
- (43). Donlan RM Biofilms: Microbial Life on Surfaces. *Emerg. Infect. Dis.* 2002, 8 (9), 881–890. [PubMed: 12194761]
- (44). Cornelis P; Dingemans J *Pseudomonas Aeruginosa* Adapts Its Iron Uptake Strategies in Function of the Type of Infections. *Front. Cell. Infect. Microbiol.* 2013, 3, 75. [PubMed: 24294593]
- (45). Diggle SP; Mattheijs S; Wright VJ; Fletcher MP; Chhabra SR; Lamont IL; Kong X; Hider RC; Cornelis P; Cámara M; Williams P The *Pseudomonas Aeruginosa* 4-Quinolone Signal Molecules HHQ and PQS Play Multifunctional Roles in Quorum Sensing and Iron Entrapment. *Chem. Biol.* 2007, 14 (1), 87–96. [PubMed: 17254955]
- (46). Kang D; Kirienko DR; Webster P; Fisher AL; Kirienko NV Pyoverdine, a Siderophore from *Pseudomonas Aeruginosa*, Translocates into *C. Elegans*, Removes Iron, and Activates a Distinct Host Response. *Virulence* 2018, 9 (1), 804–817. [PubMed: 29532717]
- (47). Cox CD Effect of Pyochelin on the Virulence of *Pseudomonas Aeruginosa*. *Infect. Immun.* 1982, 36 (1), 17–23. [PubMed: 6804387]
- (48). Lépine F; Milot S; Déziel E; He J; Rahme LG Electrospray/mass Spectrometric Identification and Analysis of 4-Hydroxy-2-Alkylquinolines (HAQs) Produced by *Pseudomonas Aeruginosa*. *J. Am. Soc. Mass Spectrom.* 2004, 15 (6), 862–869. [PubMed: 15144975]
- (49). Bredenbruch F; Nimitz M; Wray V; Morr M; Müller R; Häussler S Biosynthetic Pathway of *Pseudomonas Aeruginosa* 4-Hydroxy-2-Alkylquinolines. *J. Bacteriol.* 2005, 187 (11), 3630–3635. [PubMed: 15901684]
- (50). Wang Y; Wilks JC; Danhorn T; Ramos I; Croal L; Newman DK Phenazine-1-Carboxylic Acid Promotes Bacterial Biofilm Development via Ferrous Iron Acquisition. *J. Bacteriol.* 2011, 193 (14), 3606–3617. [PubMed: 21602354]
- (51). Dow JM; Crossman L; Findlay K; He Y-Q; Feng J-X; Tang J-L Biofilm Dispersal in *Xanthomonas Campestris* Is Controlled by Cell-Cell Signaling and Is Required for Full Virulence to Plants. *Proc. Natl. Acad. Sci. U. S. A.* 2003, 100 (19), 10995–11000. [PubMed: 12960398]
- (52). Rossmann FS; Racek T; Wobser D; Puchalka J; Rabener EM; Reiger M; Hendrickx APA; Diederich A-K; Jung K; Klein C; Huebner J Phage-Mediated Dispersal of Biofilm and Distribution of Bacterial Virulence Genes Is Induced by Quorum Sensing. *PLoS Pathog.* 2015, 11 (2), e1004653. [PubMed: 25706310]
- (53). Uppuluri P; Chaturvedi AK; Srinivasan A; Banerjee M; Ramasubramaniam AK; Köhler JR; Kadosh D; Lopez-Ribot JL Dispersion as an Important Step in the *Candida Albicans* Biofilm Developmental Cycle. *PLoS Pathog.* 2010, 6 (3), e1000828. [PubMed: 20360962]
- (54). Hay AJ; Zhu J Host Intestinal Signal-Promoted Biofilm Dispersal Induces *Vibrio Cholerae* Colonization. *Infect. Immun.* 2015, 83 (1), 317–323. [PubMed: 25368110]

- (55). Connolly KL; Roberts AL; Holder RC; Reid SD Dispersal of Group A Streptococcal Biofilms by the Cysteine Protease SpeB Leads to Increased Disease Severity in a Murine Model. *PLoS One* 2011, 6 (4), e18984. [PubMed: 21547075]
- (56). Desbois AP; Coote PJ Wax Moth Larva (*Galleria Mellonella*): An in Vivo Model for Assessing the Efficacy of Antistaphylococcal Agents. *J. Antimicrob. Chemother.* 2011, 66 (8), 1785–1790. [PubMed: 21622972]
- (57). Kaplan EL; Meier P Nonparametric Estimation from Incomplete Observations. *J. Am. Stat. Assoc.* 1958, 53 (282), 457–481.
- (58). Bland JM; Altman DG The Logrank Test. *BMJ* 2004, 328 (7447), 1073. [PubMed: 15117797]
- (59). Benjamini Y; Hochberg Y Controlling the False Discovery Rate: A Practical and Powerful Approach to Multiple Testing. *J. R. Stat. Soc. Series B Stat. Methodol.* 1995, 57 (1), 289–300.
- (60). Adler C; Corbalán NS; Seyedsayamdost MR; Pomares MF; de Cristóbal RE; Clardy J; Kolter R; Vincent PA Catechol Siderophores Protect Bacteria from Pyochelin Toxicity. *PLoS One* 2012, 7 (10), e46754. [PubMed: 23071628]

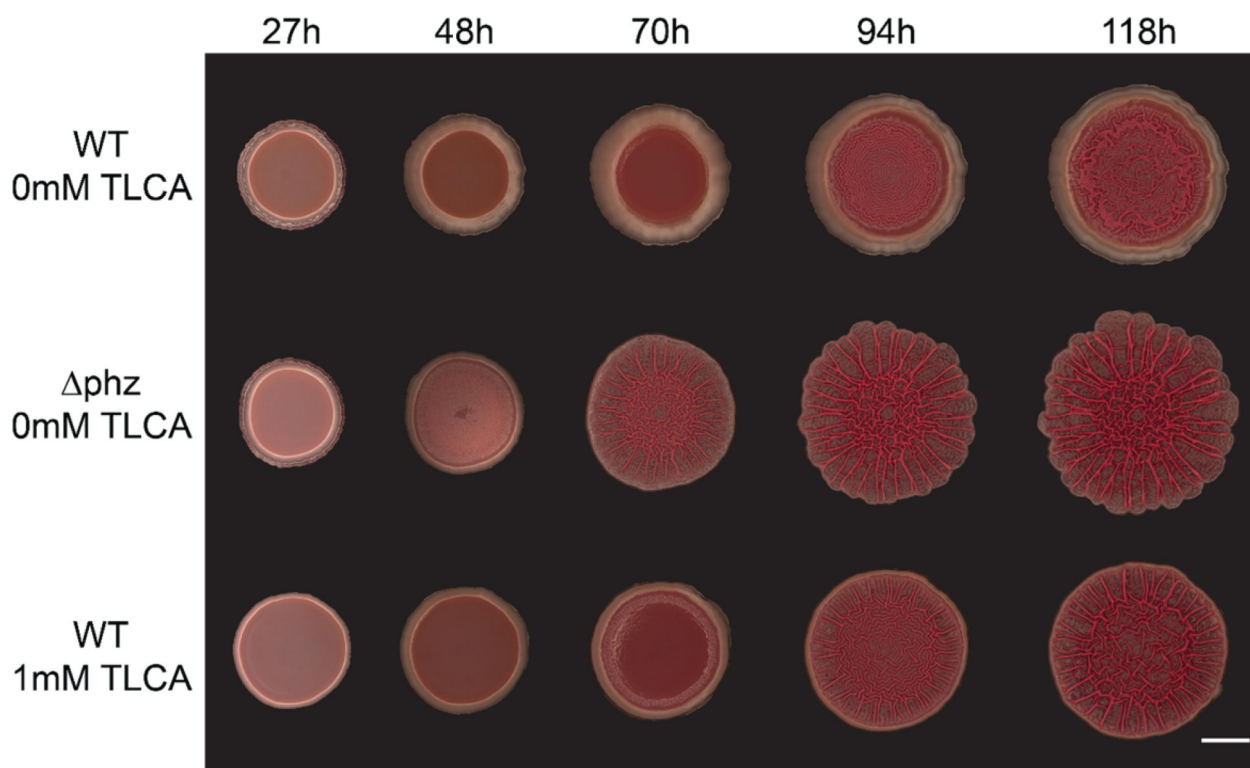


Figure 1: The effect of TLCA on colony biofilm formation in *P. aeruginosa* PA14. After five days of growth, colonies that were exposed to TLCA showed a similar hyper-wrinkled biofilm structure to that of the untreated *phz* mutant. (N =3)

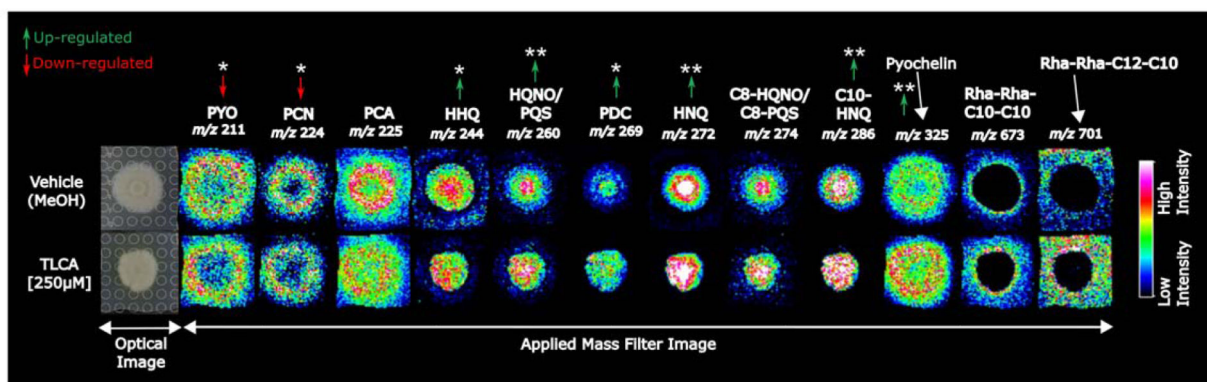


Figure 2:
MALDI-TOF IMS analysis of *P. aeruginosa* after exposure to TLCA. Twelve specialized metabolites produced by *P. aeruginosa* were identified and visualized. Signal intensity is displayed as a heat map and shows that exposure to TLCA altered regulation of highlighted specialized metabolites compared to control. * denotes the signal is significantly up- or down-regulated in two biological replicates within the colony and ** denotes the signal was significant over all three biological replicates (p<0.05).

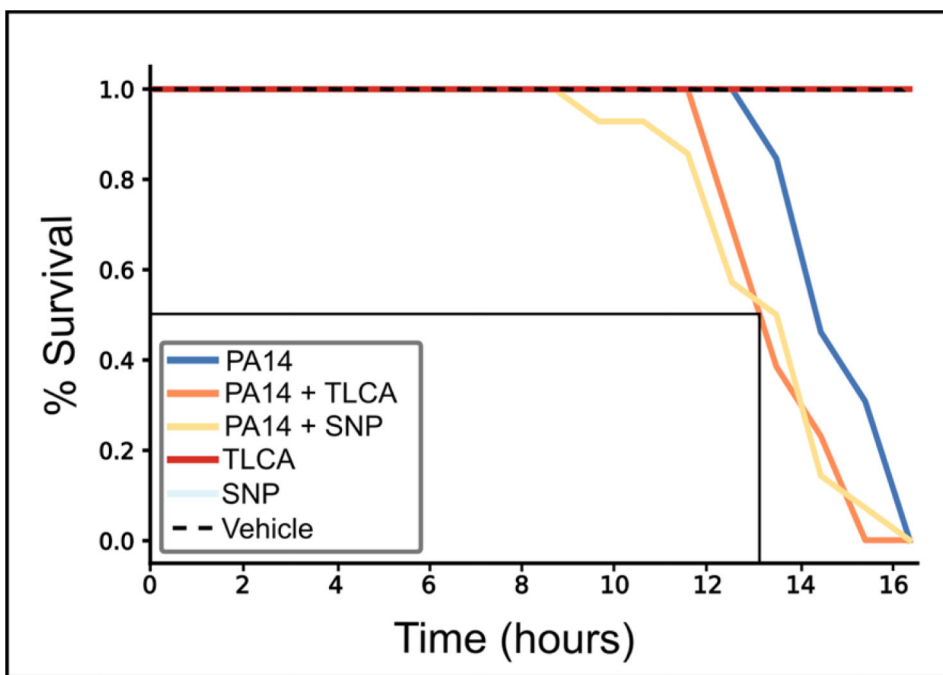


Figure 3: Virulence assay with *Galleria mellonella* (greater wax moth). Using *G. mellonella* as an infection model revealed that regardless of agent (250 μ M), WT PA14 treated cells show a significant increase in virulence compared to controls (N=3).

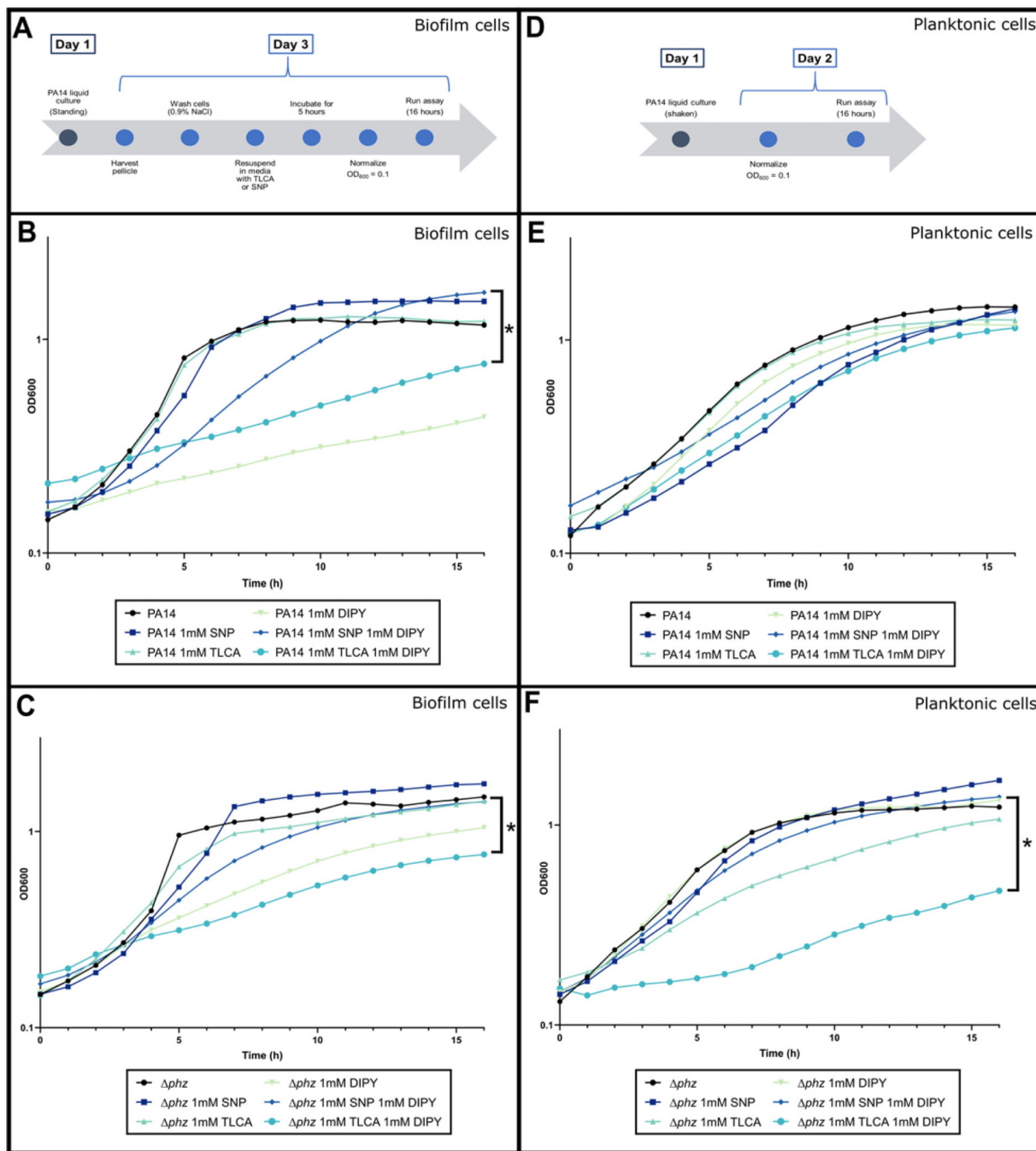


Figure 4: PA14 Iron starvation assay.

(A) Experimental workflow for collection and dispersion of PA14 biofilm cells. (B) Starvation of iron via exposure to DIPY showed that TLCA dispersed cells are more sensitive to iron starvation than SNP dispersed cells. However, cells dispersed with either agent are not more sensitive to iron starvation when compared to DIPY control. (C) The *phz* mutant dispersed cells hold the same trend with no significant change in sensitivity from TLCA or SNP treatment. (D) Experimental workflow for the preparation of planktonic cells. (E) Planktonic PA14 cells also show no sensitivity to iron starvation regardless of

agent used. (F) Interestingly, treatment of the *phz* mutant with TLCA lead to a significant increase in sensitivity to iron starvation and the population was unable to fully recover over the 16 hour experiment. * denotes $p < 0.05$.

Author Manuscript

Author Manuscript

Author Manuscript

Author Manuscript

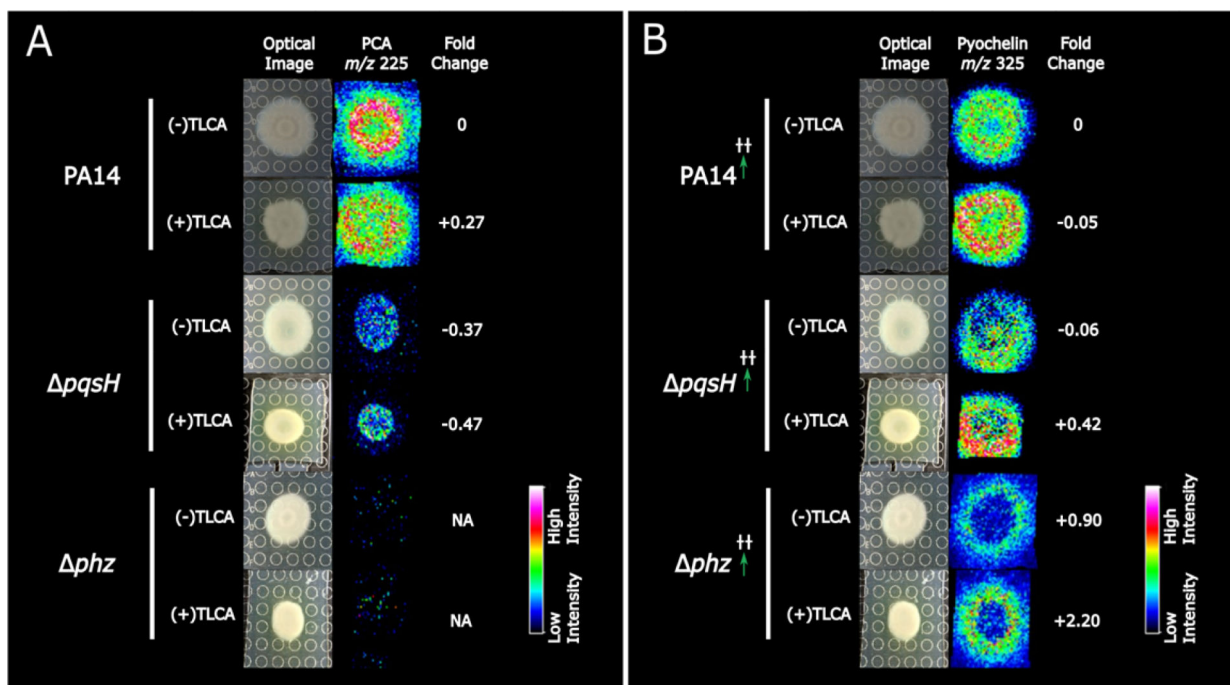


Figure 5: IMS and fold change analysis of wild type PA14, *pqsH*, and *phz* mutants. (A) IMS and HPLC fold-change analysis revealed a 250 μ M treatment of TLCA induced no change in PCA production however (B) there was an increase in pyochelin production in the *phz* mutant, resembling the trend observed in WT. †† denotes the observed regulation was statistically significant over three biological replicates in IMS experiments ($p < 0.05$).

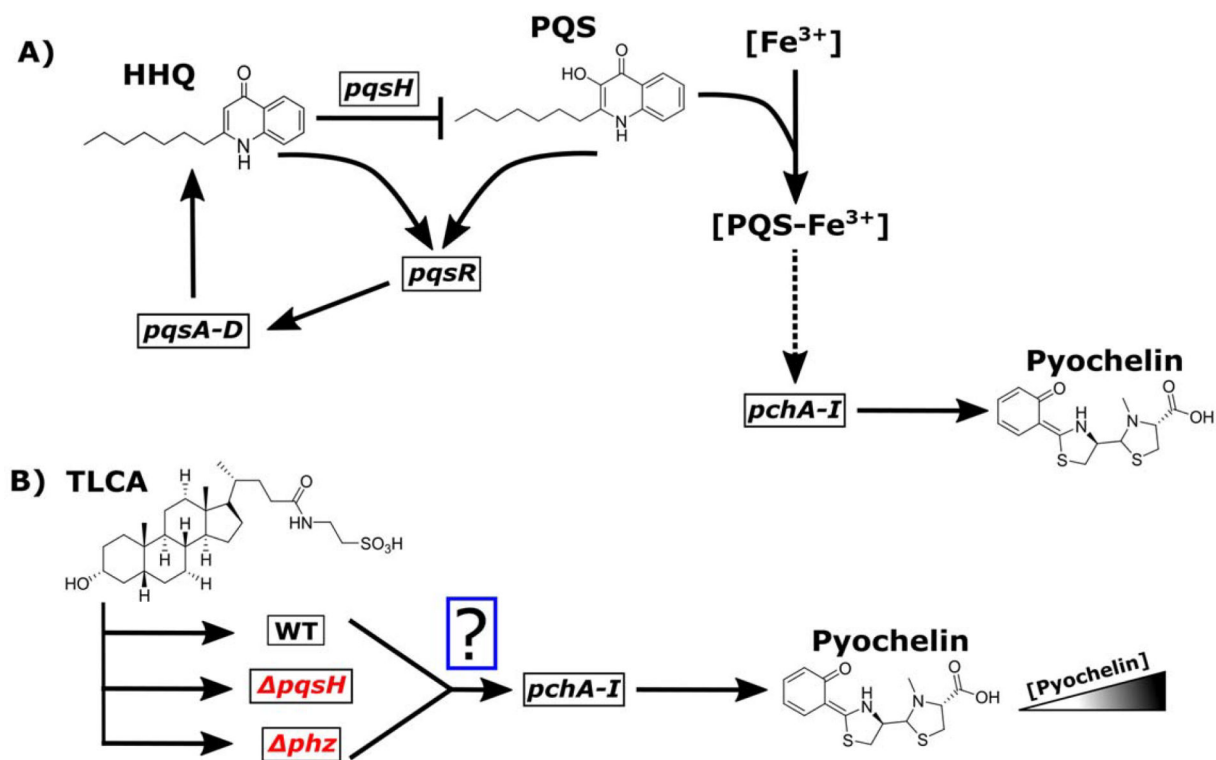


Figure 6: *pqs* metabolic pathway under TLCA exposure.

(A) Represents the canonical pathway for pyochelin production with the role iron-bound PQS plays in indirectly (dashed-line) activating pyochelin production. (B) However, TLCA treatment of the WT or *pqsH*, and *phz* mutants leads to an increase in pyochelin production and subsequently virulence supporting that these genes play a role in the observed increase in pyochelin production from TLCA exposure.